Hindawi Publishing Corporation
Journal of Nanomaterials
Volume 2010, Article ID 503186, 7 pages
doi:10.1155/2010/503186

Research Article

Growth of 1-D TiO_2 Nanowires on Ti and Ti Alloys by Oxidation

Huyong Lee,[1] Suliman Dregia,[1] Sheikh Akbar,[1] and Mansour Alhoshan[2]

[1] *Department of Materials Science and Engineering, The Ohio State University, Columbus, OH 43210, USA*
[2] *Department of Chemical Engineering, King Abdullah Institute for Nanotechnology, King Saud University, Riyadh 11421, Saudi Arabia*

Correspondence should be addressed to Sheikh Akbar, akbar.1@osu.edu

Received 27 July 2010; Accepted 11 November 2010

Academic Editor: Zhi Li Xiao

The growth of titania nanowires by a simple metal oxidation process was investigated for both commercially pure α-Ti and Ti alloys including Ti64 and β-Ti under a limited supply of oxygen. The effects of processing variables including heat treatment temperature, gas flow rate, and process duration on the growth of nanowires were explored. Similarities and differences in the growth of nanowires on pure Ti versus Ti alloys were observed. While the growth window in terms of temperature and flow rate is narrow in pure Ti, the window is much wider in the alloys. However, the trend towards high temperature is similar in all the samples promoting faceted oxide crystal growth rather than nanowires.

1. Introduction

Titanium dioxide (TiO_2) is an important inorganic compound that is widely used as a representative white pigment for plastics, paints, rubbers, cosmetics, man-made fibers, papers, and ceramics. TiO_2 has the highest refractive index which is even greater than diamond. With unique ability to reflect light, TiO_2 is used to impart whiteness, brightness, and opacity to various end-use products.

Recently, new products utilizing photocatalytic properties [1–6] of TiO_2 are being developed around the world, and the relevant market size is projected to grow significantly. TiO_2 has also received considerable attention for chemical sensing applications, especially high temperature gas sensors [7]. Dye-sensitized solar cells [8, 9], anodes of Li-based batteries [10–12], biosensors [13, 14], and biocompatible materials for bone implants [15–17] are also important applications for TiO_2. For these applications, surface area is very important to enhance the chemical and electrical properties, and nanomaterials and nanostructures offer an opportunity to enhance these properties.

To date, chemically synthesized nanoparticles have been generally used to enhance the surface area of TiO_2. More recently, one dimensional (1-D) TiO_2 nanostructures such as nanowires and nanotubes have been developed that provide high surface area, which would guarantee a high density of active sites available for surface reactions. To be able to grow 1-D structures such as nanowires, it is necessary to confine the growth direction to one dimension. This can be accomplished by either physical confinement, such as a template or by chemical adsorption confinements [18]. Literature reports TiO_2 nanostructures produced by template-directed method [19–26], electrospinning [27, 28], photoelectrochemical etching [29, 30], anodization [31–33], and hydrothermal techniques [34, 35].

Widespread utilization of nanostructured TiO_2 is often hindered by the conflicting demands for (i) precise control of fine, well-ordered surface features and (ii) low-cost, rapid mass production. Most wet chemical processes like template-directed synthesis of nanostructure require many chemical steps which increase production costs. In addition, variables such as temperature and pH should be well controlled in each chemical step. Moreover, nanostructured TiO_2 has to possess high crystallinity for most applications. TiO_2 nanotubes/nanowires produced by anodization and electrospinning are amorphous after synthesis. For photocatalytic application, crystallinity is very important since amorphous state provides lots of trap sites at which photogenerated charge carriers recombine. Additional heat treatment required for crystallization of the amorphous phase may lead to collapse of the nanostructure due to sintering and grain growth.

Growth of 1-D nanostructures can occur in many ways. One of the more popular methods is to introduce a constituent species in the gas phase. This gaseous specie then reacts with a material in the solid form, a second constituent specie in the vapor phase, or simply condenses on a surface to create nanostructures. Vapor-phase-assisted growth is one of the most common means for producing nanostructures, often nanowires, on a desired substrate. The vapor phase constituent is a metal as is the case with vapor-solid (VS) and vapor-liquid-solid (VLS) methods.

Two methods are typically used to produce the vaporized metal. The simplest method utilizes the substrate, upon which the nanostructure grows, as the source for the vapor phase. This requires a temperature high enough to produce a sufficient vapor pressure of the material. The vapor phase then condenses onto the substrate on preferential sites allowing for growth to occur. An alternative way to produce the required vapor phase is to utilize a metal source upstream from the substrate. Again, a high temperature is necessary to produce the sufficient vapor pressure to allow for downstream condensation. This method requires a rather large temperature gradient between the vapor source and the target substrate to allow for both vaporization and condensation in the same reaction vessel. While this method has been successfully used to produce nanostructures of SnO_2 and ZnO, this has not been successful for TiO_2 because of low vapor pressure of Ti.

Recent work in the authors' laboratory has led to the development of a novel and inexpensive technique that creates oriented nanofiber arrays of single-crystal TiO_2 by gas phase reaction with hydrogen [36]. While most 1-D nanostructures are created by deposition or growth [37–39], the TiO_2 nanofibers are created by etching TiO_2 grains by hydrogen-containing species (H_2/N_2 heat treatment). As oxygen from TiO_2 is taken out as H_2O (g), Ti diffuses from the surface to the bulk [40]. We have also developed a method involving H_2/N_2 heat treatment to grow nanofibers of SnO_2 in parts of the sample coated with gold, showing directional growth on grains with crystal facets [41]. The top end of each growing SnO_2 nanofiber contained a gold nanoparticle, with a distinct orientation relation detected at the Au/SnO_2 interface. Solid-state and/or gas phase diffusion paths provided possible mechanisms of mass transport of tin and oxygen from the substrate to the ends of the nanofibers for sustained nanofiber growth. Unlike previous vapor-solid or vapor-liquid-solid processes for forming single crystal SnO_2 nanofibers, this hydrogen-induced surface rearrangement process did not require a separate Sn-O vapor source located upstream of the substrate. More recently, we have developed a process to create nanofibers of TiO_2 on Ti and Ti alloys via the oxidation process under a limited supply of oxygen in an Ar environment. The fiber diameters are in the range of 50–80 nm (controlled by the temperature) and of the length of ~1–10 μm (controlled by the reaction time) [42].

What is common to these structures is that they are created without the use of lithography and involve a gas-phase reaction. Thus, these methods provide an economical way to mass-produce high-surface area ceramic nanostructures that are attached to a substrate. This makes them ideal platforms with catalytic, gas-sensing, electronic, and antimicrobial functions for a variety of chemical manufacturing, environmental, transportation, and biomedical applications. The focus of this paper is on the synthesis of 1-D nano-structured TiO_2 on Ti and Ti alloys using the oxidation process under a limited supply of oxygen (10 s to 100 s of ppm level) similar to that reported in [42]. Ar gas was flown into the furnace from a laboratory grade Ar cylinder. Oxidation-driven nanowire growth of TiO_2 and their applications in electroemission and cell repellence have recently been reported in literature [43–45]. While in these reported cases the oxidation was carried out in an acetone saturated Ar environment, what we report here is a simpler process since it is done in Ar alone.

2. Experimental

Commercially pure Ti (grade 2), Ti64 (grade 5, Ti-6 wt% Al-4 wt% V; Onlinemetals, Seattle, WA), and β-Ti (Ti-5 wt% Al-5 wt% V-5 wt% Mo-3.5 wt% Cr-0.5 wt% Fe; referred to as β-Ti(5-5-5)) bars were used for the experiments. Samples from bars were cut using a diamond cutter (LECO, part number 801-136) and mechanically polished using SiC sand paper. The samples were ultrasonicated for 5 minutes in acetone and methanol and rinsed in DI (deionized) water. The samples were then immersed into a bath of 30 wt% of HCl in DI water for 10 minutes at 80°C to gently remove native oxide layers, and then residual water droplets were blown away by an air gun and dried out for 1 day.

The samples were then inserted into a quartz tube which was placed in a horizontal tube furnace (Lindberg, TF55035A) for gas heat treatments. The tube was first purged with 5% H_2 balanced with Ar gas flown at a rate of 1000 mL/min for 1 hr. Then the temperature of the furnace was raised at 30°C/min and maintained at the target temperature (700–900°C) for a certain time period (6–10 hr) with three different Ar gas flow rates: 200, 500, and 1000 mL/min. The flow rate of Ar was maintained by a manual gas flowmeter, and the oxygen partial pressure in the gas was monitored by an oxygen sensor (CG-1000, AMTEK). The humidity was also monitored by a humidity sensor (HMP234, Vaisala), and the level of the humidity was maintained at approximately 0.5% relative humidity. The value of the oxygen concentration in the Ar gas ranged from 10 s to 100 s of ppm throughout the heat treatment process. The sample was cooled down to room temperature rapidly by air quenching to enhance cooling of the sample and to minimize unnecessary oxidation during cooling.

Field emission scanning electron microscope (FEG-SEM, Model XL-30, Philips) was used to characterize the surface morphology of the metal specimens before and after exposure to the Ar gas treatment. A Sirion SEM (FEG-SEM, Model Sirion, FEI, Oregon) was used for high-resolution observation to detect changes in the surface morphology of the specimens at submicron scales. For the SEM observation, a thin layer of gold was deposited on the heat-treated samples to avoid charging effect.

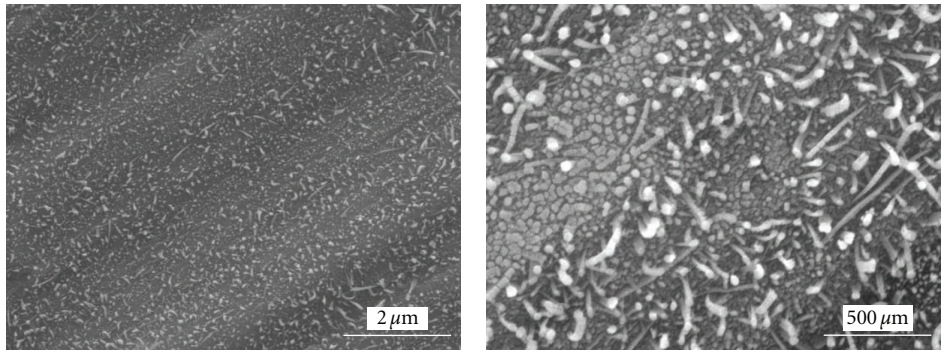

(a) (b)

Figure 1: SEM image of pure α-Ti sample heat-treated in Ar gas containing 10 s to 100 s of ppm of oxygen at 600°C for 8 hr at a flow rate of 200 mL/min; (a): low magnification and (b): higher magnification.

3. Results and Discussions

3.1. Pure α-Ti. Exposure of pure Ti to Ar gas containing ~ppm of oxygen at a flow rate of 200 mL/min for 8 hours at 600°C resulted in the growth of TiO_2 nanowires. The length of nanowires is in the range of 50 nm to 400 nm as represented in Figure 1. The flow rate was changed to observe its effect on the growth of nanowires. An increase in the flow rate from 200 mL/min to 1000 mL/min caused the disappearance of the nanowires. The effect of the flow rate was more obvious as the temperature for the heat treatment was increased. Higher flow rate and higher temperature promoted growth of faceted oxide crystals and platelets. Hence, the window of high aspect ratio nanowire growth was found to be very narrow in pure Ti, as illustrated in Figure 2. The phase of nanowire in this case as well as all those reported in this paper was confirmed to be rutile by electron diffraction in a TEM.

Even though the relationship between the flow rate and the change of morphology on the surface has been reported in literature, there is no clear understanding of the effect in these reports [46–48]. By combining experiments of nanostructure growth by oxidation of Cu foil in combination with computer simulation of the gas flux, Xu et al. [46] showed that in an area of higher flux, a higher oxygen concentration was present which promoted nanowire growth only in these areas. According to Peng and Chen [47], the use of a gas environment containing a lower concentration of oxygen was required for the growth of titania nanowires from pure Ti, which is contradictory to the results of the growth of nanowires from Cu oxidation, but consistent with our observation.

To understand the effect of the flow rate, it is useful to determine the gas flow pattern across the sample. The Reynolds number was calculated to determine the pattern of the gas flow with a reference value of 2100 [49]. Values above 2100 indicate turbulent gas flow while numbers less than 2100 indicate laminar or viscous flow. The calculated Reynolds number for our experiments was ~20 indicating that the gas flow in the quartz tube was laminar. When the flow rate is changed in a laminar flow, the convection layer thickness defined by the following equation also changes:

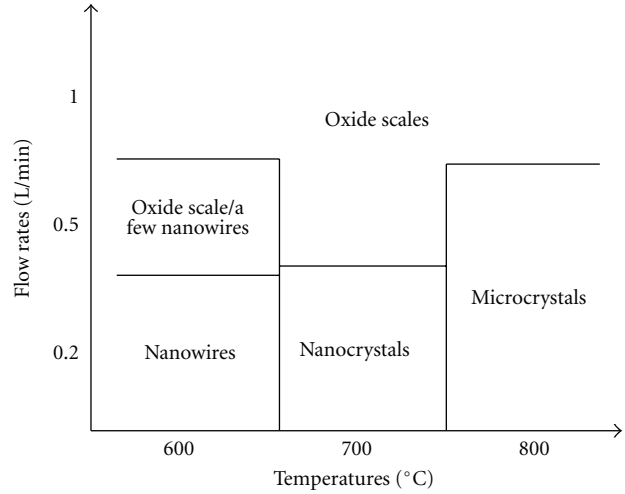

Figure 2: Processing map with resultant structures in pure α-Ti. Temperatures used: 600, 700, and 800°C. Flow rates used: 200, 500, and 1000 mL/min.

$$\delta = 5.0\left(\frac{\upsilon_{\text{ki}}}{\nu_{\text{gas}}}\right)^{0.5}\chi^{0.5}, \quad (1)$$

where υ_{ki} is the kinematic viscosity of the gas, ν_{gas} is the velocity of the gas, and χ is the distance from the leading edge of the sample. Based on (1), the reaction boundary layer thickness decreases as the flow rate increases. The gas reaction boundary layer thicknesses at flow rates of 200 mL/min and 1000 mL/min, with the center of the sample being 2.5×10^{-3} m from the edge, are calculated to be 0.02 m and 0.0089 m, respectively. At a lower flow rate of 200 mL/min, the increased gas reaction layer thickness causes oxygen to transfer slowly to the surface of the substrate, and this slowed oxygen supply preferentially promotes the formation of nanowires over a continuous oxide layer.

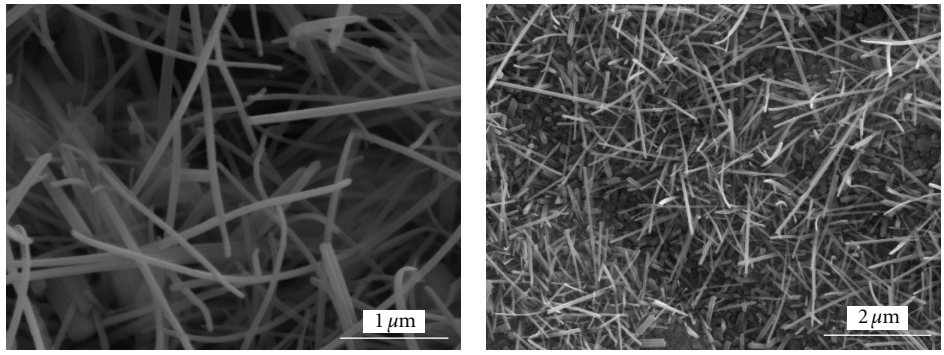

(a) (b)

Figure 3: SEM images of the heat-treated samples, (a): Ti64 and (b): β-Ti (5-5-5). The heat treatment temperature was 700°C for 8 hr at a flow rate of 1000 mL/min.

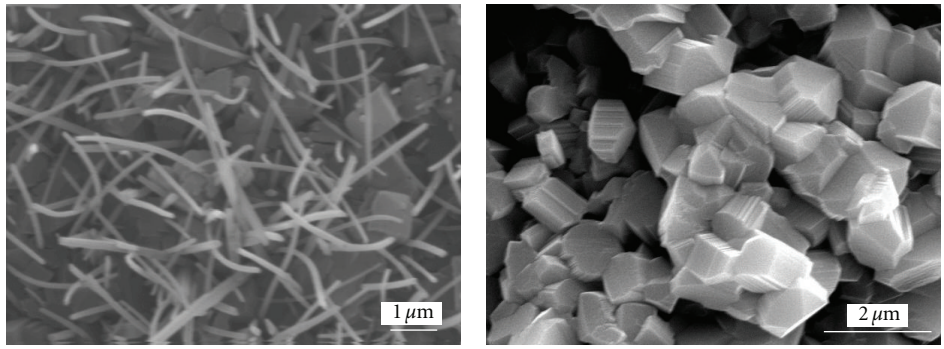

(a) (b)

Figure 4: SEM images of (a) Ti64 heat treated at 800°C showing a mixture of nanowires and faceted crystals and (b) β-Ti (5-5-5) heat treated at 900°C showing faceted equiaxed crystals only.

3.2. Ti Alloys. Pure Ti (α phase) transforms to β phase at 880°C [50]. There are no pure β-Ti alloys below the transition temperature which do not contain β stabilizers such as V, Mo, and Cr. As a result, separating the impact of stabilizing elements from the β phase in nanofiber formation becomes very complicated. When Ti64 and β-Ti samples were heat treated at 700°C for 8 hr with various flow rates, nanowires were formed all over the surface as shown in Figures 3(a) and 3(b). The difference between Ti64 and β-Ti (5-5-5) is the amount of β phase and chemical compositions. Usually, Ti64 is a mixture of α and β phases with the β phase existing as lamellar structures in the domain of α phase.

A change in the flow rate did not show any dramatic effect on the growth of nanowires for both Ti64 and β-Ti (5-5-5). However, the effect of temperature was similar to the general trend observed in α-Ti. While 700°C was found optimum for nanowire growth in the alloys, 800°C produced a mixture of well-faceted crystals and nanowires (Figure 4(a)), and 900°C produced well-faceted equiaxed crystals and platelets (Figure 4(b)) only. This general trend towards high temperature seems to indicate that 1-D growth at low temperature is driven by oxidation reaction anisotropy with preferential growth on certain crystal faces. This anisotropy decreases at higher temperature promoting growth on other surfaces leading to facetted crystals. Details of the growth mechanism will be the focus of another publication.

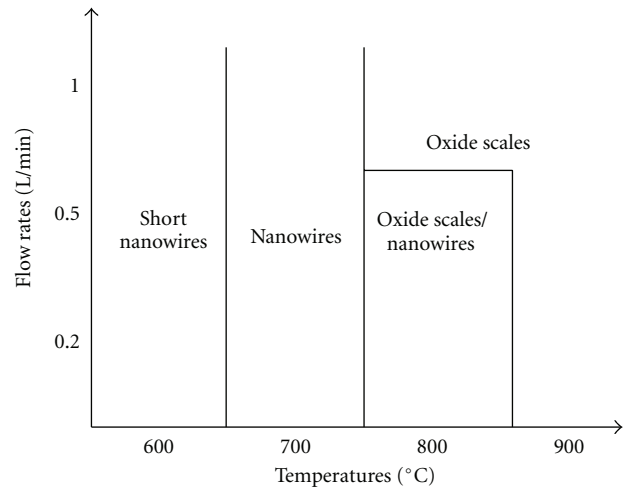

Figure 5: Processing map with resultant structures for Ti64 and β-Ti (5-5-5) alloys. Temperature used: 600, 700, 800, and 900°C. Flow rates used: 200, 500, and 1000 mL/min.

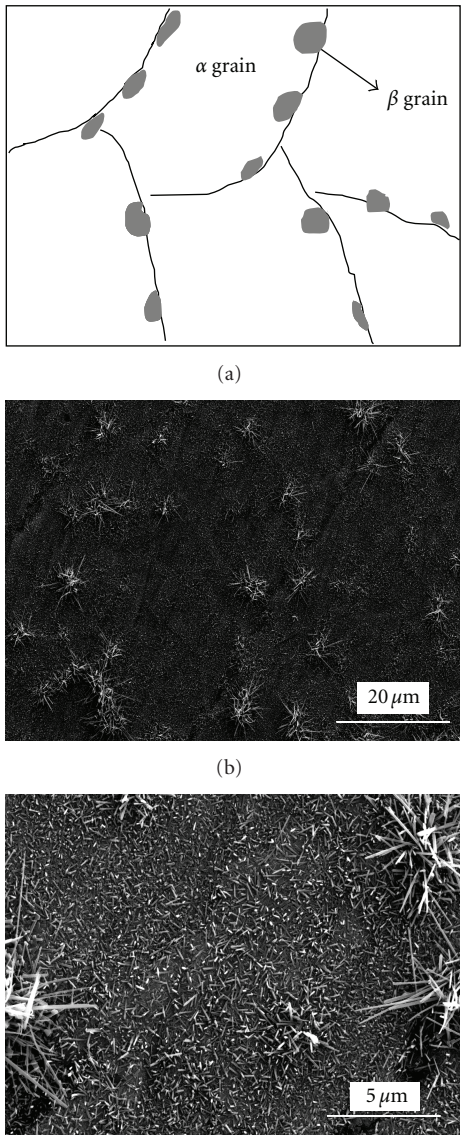

(a)

(b)

(c)

Figure 6: (a) A schematic diagram of Ti alloy samples showing the β precipitates along the grain boundary of the α-matrix, (b) a surface image of the alloy sample after the heat treatment at 700°C for 8 hr at a flow rate of 500 mL/min, and (c) the image at higher magnification highlighting enhanced growth around the β phase.

Compared to α-Ti, in Ti alloys the growth window was found to be much wider as illustrated in Figure 5. From these results, it is apparent that samples containing the β phase are much better suited for nanowire formation by the oxidation process.

To identify the dependence of nanowire formation on each phase more clearly, Ti-6.85 wt% Al-1.6 wt% V with a specific microstructure was used for the heat treatment. A schematic diagram of the microstructure of this sample is represented in Figure 6(a). The β phase lies only along the grain boundaries of the α phase. The sample was heat treated at 700°C for 8 hr at a flow rate of 500 mL/min, the results of which are shown in Figures 6(b)-6(c). Nanowire formation was achieved across the sample; however, both the length and density of the nanowires were enhanced at locations containing the β phase.

4. Conclusions

Growth of nanowires was observed on the surfaces of commercially pure α-Ti as well as Ti64 and β-Ti(5-5-5) alloys using a high temperature heat treatment in Ar gas containing ~ppm of oxygen. The growth window in α-Ti was narrow and limited to low temperature (600°C) and low flow rate (200 mL/min). The growth window in Ti64 and β-Ti(5-5-5) alloys was much wider with flow rate having no dramatic effect. In the alloys, while the optimum growth temperature was 700°C, a mixture of nanowires and faceted crystals was produced at 800°C, and 900°C produced faceted equiaxed crystals only. High temperature promoted faceted crystal growth in α-Ti as well. This general trend towards high temperature seems to indicate that 1-D growth at low temperature is driven by oxidation reaction anisotropy with preferential growth on certain crystal faces. This anisotropy decreases at higher temperature promoting growth on other surfaces leading to facetted equiaxed crystals.

Acknowledgment

Publication charges for this paper was paid by King Saud University in Riyadh, Saudi Arabia.

References

[1] T. Inoue, A. Fujishima, S. Konishi, and K. Honda, "Photoelectrocatalytic reduction of carbon dioxide in aqueous suspensions of semiconductor powders," *Nature*, vol. 277, no. 5698, pp. 637–638, 1979.

[2] T. Kawai and T. Sakata, "Conversion of carbohydrate into hydrogen fuel by a photocatalytic process," *Nature*, vol. 286, no. 5772, pp. 474–476, 1980.

[3] G. N. Schrauzer and T. D. Guth, "Photolysis of water and photoreduction of nitrogen on titanium dioxide," *Journal of the American Chemical Society*, vol. 99, no. 22, pp. 7189–7193, 1977.

[4] S. Sato and J. M. White, "Photoassisted hydrogen production from titania and water," *Journal of Physical Chemistry*, vol. 85, no. 5, pp. 592–594, 1981.

[5] S. Matsuda and A. Kato, "Titanium oxide based catalysts—a review," *Applied Catalysis*, vol. 8, no. 2, pp. 149–165, 1983.

[6] Y. Nakato, H. Akanuma, J. I. Shimizu, and Y. Magari, "Photo-oxidation reaction of water on an n-TiO_2 electrode. Improvement in efficiency through formation of surface micropores by photo-etching in H_2SO_4," *Journal of Electroanalytical Chemistry*, vol. 396, no. 1-2, pp. 35–39, 1995.

[7] L. D. Birkefeld, A. M. Azad, and S. A. Akbar, "Carbon monoxide and hydrogen detection by anatase modification of titanium dioxide," *Journal of the American Ceramic Society*, vol. 75, pp. 2964–2968, 1992.

[8] A. Hagfeld and M. Grätzel, "Light-induced redox reactions in nanocrystalline systems," *Chemical Reviews*, vol. 95, no. 1, pp. 49–68, 1995.

[9] B. O'Regan and M. Grätzel, "A low-cost, high-efficiency solar cell based on dye-sensitized colloidal TiO_2 films," *Nature*, vol. 353, no. 6346, pp. 737–740, 1991.

[10] M. Wagemaker, A. P.M. Kentjens, and F. M. Mulder, "Equilibrium lithium transport between nanocrystalline phases in intercalated TiO_2 anatase," *Nature*, vol. 418, no. 6896, pp. 397–399, 2002.

[11] C. Natarajan, K. Setoguchi, and G. Nogami, "Preparation of a nanocrystalline titanium dioxide negative electrode for the rechargeable lithium ion battery," *Electrochimica Acta*, vol. 43, no. 21-22, pp. 3371–3374, 1998.

[12] C. Natarajan, N. Fukunaga, and G. Nogami, "Titanium dioxide thin film deposited by spray pyrolysis of aqueous solution," *Thin Solid Films*, vol. 322, no. 1-2, pp. 6–8, 1998.

[13] Q. Li, G. Luo, J. Feng, Q. Zhou, LI. Zhang, and Y. Zhu, "Amperometric detection of glucose with glucose oxidase absorbed on porous nanocrystalline TiO_2 film," *Electroanalysis*, vol. 13, no. 5, pp. 413–416, 2001.

[14] Q. Li, G. Luo, and J. Feng, "Direct electron transfer for heme proteins assembled on nanocrystalline TiO_2 film," *Electroanalysis*, vol. 13, no. 5, pp. 359–363, 2001.

[15] J. X. Liu, D. Z. Yang, F. Shi, and Y. J. Cai, "Sol-gel deposited TiO_2 film on NiTi surgical alloy for biocompatibility improvement," *Thin Solid Films*, vol. 429, no. 1-2, pp. 225–230, 2003.

[16] G. Giavaresi, L. Ambrosio, G. A. Battiston et al., "Histomorphometric, ultrastructural and microhardness evaluation of the osseointegration of a nanostructured titanium oxide coating by metal-organic chemical vapour deposition: an in vivo study," *Biomaterials*, vol. 25, no. 25, pp. 5583–5591, 2004.

[17] M. Keshmiri and T. Troczynski, "Apatite formation on TiO_2 anatase microspheres," *Journal of Non-Crystalline Solids*, vol. 324, no. 3, pp. 289–294, 2003.

[18] B. Dinan and S. A. Akbar, "One dimensional oxide nanostructures by gas phase reaction," *Functional Materials Letters*, vol. 2, no. 3, pp. 87–94, 2009.

[19] S. Z. Chu, K. Wada, S. Inoue, S. I. Hishita, and K. Kurashima, "Fabrication and structural characteristics of ordered TiO_2-Ru(-RuO_2) nanorods in porous anodic alumina films on ITO/glass substrate," *Journal of Physical Chemistry B*, vol. 107, no. 37, pp. 10180–10184, 2003.

[20] S. Inoue, S. Z. Chu, K. Wada, DI. Li, and H. Haneda, "New roots to formation of nanostructures on glass surface through anodic oxidation of sputtered aluminum," *Science and Technology of Advanced Materials*, vol. 4, no. 4, pp. 269–276, 2003.

[21] L. Miao, S. Tanemura, S. Toh, K. Kaneko, and M. Tanemura, "Fabrication, characterization and Raman study of anatase-TiO_2 nanorods by a heating-sol-gel template process," *Journal of Crystal Growth*, vol. 264, no. 1–3, pp. 246–252, 2004.

[22] M. Zhang, Y. Bando, and K. Wada, "Sol-gel template preparation of TiO_2 nanotubes and nanorods," *Journal of Materials Science Letters*, vol. 20, no. 2, pp. 167–170, 2001.

[23] S. Lee, C. Jeon, and Y. Park, "Fabrication of TiO_2 tubules by template synthesis and hydrolysis with water vapor," *Chemistry of Materials*, vol. 16, no. 22, pp. 4292–4295, 2004.

[24] X. H. Li, W. M. Liu, and H. L. Li, "Template synthesis of well-aligned titanium dioxide nanotubes," *Applied Physics A*, vol. 80, no. 2, pp. 317–320, 2005.

[25] T. Peng, H. Yang, G. Chang, KE. Dai, and K. Hirao, "Synthesis of bamboo-shaped TiO_2 nanotubes in nanochannels of porous aluminum oxide membrane," *Chemistry Letters*, vol. 33, no. 3, pp. 336–337, 2004.

[26] Y. Lei, L. D. Zhang, and J. C. Fan, "Fabrication, characterization and Raman study of TiO_2 nanowire arrays prepared by anodic oxidative hydrolysis of $TiCl_3$," *Chemical Physics Letters*, vol. 338, no. 4–6, pp. 231–236, 2001.

[27] D. Li and Y. Xia, "Fabrication of titania nanofibers by electrospinning," *Nano Letters*, vol. 3, no. 4, pp. 555–560, 2003.

[28] D. Li and Y. Xia, "Direct fabrication of composite and ceramic hollow nanofibers by electrospinning," *Nano Letters*, vol. 4, no. 5, pp. 933–938, 2004.

[29] T. Sugiura, T. Yoshida, and H. Minoura, "Designing a TiO_2 nano-honeycomb structure using photoelectrochemical etching," *Electrochemical and Solid-State Letters*, vol. 1, no. 4, pp. 175–177, 1998.

[30] H. Masuda, K. Kanezawa, M. Nakao et al., "Ordered arrays of nanopillars formed by photoelectrochemical etching on directly imprinted TiO_2 single crystals," *Advanced Materials*, vol. 15, no. 2, pp. 159–161, 2003.

[31] D. Gong, C. A. Grimes, O. K. Varghese et al., "Titanium oxide nanotube arrays prepared by anodic oxidation," *Journal of Materials Research*, vol. 16, no. 12, pp. 3331–3334, 2001.

[32] O. K. Varghese, D. Gong, M. Paulose, C. A. Grimes, and E. C. Dickey, "Crystallization and high-temperature structural stability of titanium oxide nanotube arrays," *Journal of Materials Research*, vol. 18, no. 1, pp. 156–165, 2003.

[33] O. K. Varghese, D. Gong, M. Paulose, K. G. Ong, E. C. Dickey, and C. A. Grimes, "Extreme changes in the electrical resistance of titania nanotubes with hydrogen exposure," *Advanced Materials*, vol. 15, no. 7-8, pp. 624–627, 2003.

[34] T. Kasuga, M. Hiramatsu, A. Hoson, T. Sekino, and K. Niihara, "Formation of titanium oxide nanotube," *Langmuir*, vol. 14, no. 12, pp. 3160–3163, 1998.

[35] T. Kasuga, M. Hiramatsu, A. Hoson, T. Sekino, and K. Niihara, "Titania nanotubes prepared by chemical processing," *Advanced Materials*, vol. 11, no. 15, pp. 1307–1311, 1999.

[36] S. Yoo, S. A. Akbar, and K. H. Sandhage, "Nanocarving of bulk titania crystals into oriented arrays of single-crystal nanofibers via reaction with hydrogen-bearing gas," *Advanced Materials*, vol. 16, no. 3, pp. 260–264, 2004.

[37] O. K. Varghese, D. Gong, M. Paulose, C. A. Grimes, and E. C. Dickey, "Crystallization and high-temperature structural stability of titanium oxide nanotube arrays," *Journal of Materials Research*, vol. 18, no. 1, pp. 156–165, 2003.

[38] J. J. Wu and C. C. Yu, "Aligned TiO_2 nanorods and nanowalls," *Journal of Physical Chemistry B*, vol. 108, no. 11, pp. 3377–3379, 2004.

[39] D. Li and Y. Xia, "Fabrication of titania nanofibers by electrospinning," *Nano Letters*, vol. 3, no. 4, pp. 555–560, 2003.

[40] S. Yoo, S. A. Dregia, S. A. Akbar, H. Rick, and K. H. Sandhage, "Kinetic mechanism of TiO_2 nanocarving via reaction with hydrogen gas," *Journal of Materials Research*, vol. 21, no. 7, pp. 1822–1829, 2006.

[41] C. Carney, Y. Cai, S. Yoo, K. H. Sandhage, and S. A. Akbar, "Reactive conversion of microcrystalline SnO_2 into single crystal SnO_2 nanofibers at low oxygen partial pressures," *Journal of Materials Research*, vol. 23, no. 10, pp. 2639–2644, 2008.

[42] B. Dinan and S. A. Akbar, "One dimensional oxide nanostructures by gas-phase reaction," *Functional Nanomaterials Letters*, vol. 2, no. 3, pp. 87–94, 2009.

[43] K. Huo, X. Zhang, J. Fu et al., "Synthesis and field emission properties of rutile TiO_2 nanowires arrays grown directly on a ii ti metal self-source substrate," *Journal of Nanoscience and Nanotechnology*, vol. 9, no. 5, pp. 3341–3346, 2009.

[44] K. Huo, X. Zhang, L. Hu, X. Sun, J. Fu, and P. K. Chu, "One-step growth and field emission properties of quasialigned TiO_2

nanowire/carbon nanocone core-shell nanostructure arrays on Ti substrates," *Applied Physics Letters*, vol. 93, no. 1, Article ID 013105, 2008.

[45] L. Zhao, L. Hu, K. Huo, Y. Zhang, Z. Wu, and P. K. Chu, "Mechanism of cell repellence on quasi-aligned nanowire arrays on Ti alloy," *Biomaterials*, vol. 31, no. 32, pp. 8341–8349, 2010.

[46] C. Xu, X. Yang, S. Q. Shi, Y. Liu, C. Surya, and C. Woo, "Effects of local gas-flow field on synthesis of oxide nanowires during thermal oxidation," *Applied Physics Letters*, vol. 92, no. 25, Article ID 253117, 2008.

[47] X. Peng and A. Chen, "Aligned TiO_2 nanorod arrays synthesized by oxidizing titanium with acetone," *Journal of Materials Chemistry*, vol. 14, no. 16, pp. 2542–2548, 2004.

[48] X. Peng, J. Wang, D. F. Thomas, and A. Chen, "Tunable growth of TiO_2 nanostructures on Ti substrates," *Nanotechnology*, vol. 16, no. 10, pp. 2389–2395, 2005.

[49] J. G. Detry, C. Deroanne, M. Sindic, and B. B. B. Jensen, "Laminar flow in radial flow cell with small aspect ratios: numerical and experimental study," *Chemical Engineering Science*, vol. 64, no. 1, pp. 31–42, 2009.

[50] H. Okamoto, " O-Ti (oxygen-titanium)," *Journal of Phase Equilibria*, vol. 22, no. 4, p. 515, 2001.